

# THEORETICAL STUDY ON STRUCTURAL AND MECHANICAL PROPERTIES OF SINGLE LANTHANUM AND SAMARIUM ATOMS DOPED $\text{NbX}_2$ (X= S, SE) MONOLAYER

<sup>1</sup>Godwin John Ibeh, <sup>1,2</sup>Jabir Adamu Tahir, <sup>2</sup>Alhassan Shuaibu

<sup>1</sup>Department of Physics, Nigerian Defence Academy, Kaduna, Nigeria

<sup>2</sup>Department of Physics, Kaduna State University, PMB 2339, Kaduna, Nigeria

\*Corresponding Author Email Address: [gjiibeh@nda.edu.ng](mailto:gjiibeh@nda.edu.ng)

## ABSTRACT

Pure  $\text{NbX}_2$  (X=S, Se) exhibits remarkable mechanical and electronic properties; many electromechanical applications may come from chemically doping it with heteroatoms. The goal is to tune the atomic lattice and, in turn, modulate the structural properties of  $\text{NbX}_2$  (X=S, Se) – that may also affect the mechanical responses of the  $\text{NbX}_2$  (X=S, Se) monolayer. Particularly essential for both practical applications and fundamental interests is to characterize the effect of chemical doping on the mechanical properties of  $\text{NbX}_2$  (X=S, Se). Here we report  $\text{NbX}_2$  (X=S, Se) can maintain a large fraction of its pure strength and stiffness after substituting RE (La and Sm) for Nb atoms. Counter-intuitively, RE doping can ameliorate the brittle nature of the original lattice by deflecting the cracks and enabling damage-tolerant behaviors. We further offer a direct mapping between the Raman spectra and the measured mechanical performances that can show the relationship between doping structure and mechanical properties of  $\text{NbX}_2$  (X=S, Se). This work offers important implications for the rational design of  $\text{NbX}_2$  (X=S, Se) -based systems that require chemical modifications and also utilize the mechanics of  $\text{NbX}_2$  (X=S, Se).

**Keywords:** Monolayer- $\text{NbX}_2$  (X= S, Se); Density functional theory (DFT); Structural and Mechanical properties

## INTRODUCTION

Interest in two-dimensional (2D) transition metal dichalcogenides (TMDCs) has been growing in recent years, due to their unique properties and high potential for electronic and optoelectronic applications (Ostroverkhova, 2016): 2D-TMDCs are a type of low-dimensional materials with an  $\text{MX}_2$  formula, where M stands for transition metals such as Mo, W and Nb, and X stands for S, Se and Te (Ding, et al, 2011). However, the properties of 2D-TMDC are extremely monotonous and limited. 2D TMDCs hold significant potential for next-generation solar cells due to their favorable optical properties, tunable band gaps, and high charge carrier mobility, enabling the creation of ultra-thin, flexible, and efficient devices. Their integration into solar cell architectures can improve light absorption through heterostructures, facilitate charge separation, and enhance stability (Roy, & Bermel, 2018).. Common doping strategies for 2D-TMDC include substitution doping during growth, ion implantation and surface charge transfer (Leonhardt, et al.2019). However, in these previous doping regimes, the injection of ions and the transfer of surface charge in monolayer 2D-TMDC doping were often not sufficiently stable and therefore limited in their application (Ryder, et al, 2016). Substitution of 2D-TMDC doping has been extensively investigated for electronic and optoelectronic applications (Tedstone, Lewis, &

O'Brien, 2016), as well as for room temperature ferromagnetic applications (Yang et al, 2023). Transition elements are used as cationic surrogates for doped 2D-TMDCs, such as Nb ion-doped 2D-TMDCs with p-type transport properties (Tedstone, Lewis, & O'Brien, 2016), and Re ion-doped 2D-TMDCs with almost degenerate doping properties (Li, S., et al, 2021). In addition, other transition metals have been demonstrated to be viable substitutes for  $\text{NbX}_2$  (X = S) - in electronic applications studies, such as Mn (Khan, et al, 2024). The abovementioned research has shown that doping of transition metals can improve the electrical, optical, and magnetic properties of 2D-TMDCs (Iqbal, et al 2020). Recently, transition metals have been extensively demonstrated as good substitutional dopants. However, doping of atomically thin TMDCs by introducing elements with different atomic valences and atomic configurations, such as RE, is still problematic. Currently, there are a number of problematic aspects with regard to the substitution of RE elements for large monolayers of 2D-TMDF (Yoo, Heo, Ansari, & Cho, 2021).

The RE elements, which are usually found as trivalent cations, consist of 15 lanthanides (from lanthanum to lutetium), plus scandium and yttrium (Atwood, 2013). In previous studies, it has been noted that RE ions are commonly doped in traditional isolators or semiconductors (Braud, 2010). Rumour bullets may also be used as effective dispersal agents in TMDC bullets. Lanthanide (Ln) ions have a highly f-orbital configuration, which allows them to absorb and emit photons in the ultraviolet to infrared range by 4f-4f or 4f-5d transitions, and therefore they are candidates for enhanced luminescence in 2D-TMDC semiconductors (Malik, et al, 2022). In addition, RE dopants with empty 4f states and charge transfer states can provide a strong spin-orbit coupling to fine-tune the semiconductor properties of the 2D-TMDC material. In addition, first-principles calculations confirm the potential for doping 2D-TDI with rare earth elements (Rani, & Sinha, 2024).. At present, research is being conducted on RE-integrated 2D-TDMCs for optical, electronic, and magnetic applications.

$\text{NbX}_2$  (X=S, Se) was chosen as the doping host material because it is a typical example from the layered 2D-TMDC family of materials. Additionally, Sm and La are more economical compared to Er and Eu elements when considering the optimization conditions for rare-earth element-doped monolayer 2D materials, as most experimentalists agree. Hence, there is a need to know more about the effect of Sm and La doping on the mechanical and electronic properties, which, to our best knowledge, is not well understood for  $\text{NbX}_2$  (X=S, Se) monolayers.

## MATERIALS AND METHODS

In this work, La and Sm doped 2D NbX<sub>2</sub> (X=S, Se) are modeled by replacing the Nb atom in 2 × 2 × 1 supercell with La and Sm atoms. These atoms are chosen because the size of Nb atom is almost the same size as La and Sm atoms, which reduces the change in the supercell (Radzwan *et al.*, 2020). The main aim is to make the materials n-type semiconductors so they can serve as electron transport materials in a perovskite solar cell (PSC). Moreover, doping on the chalcogen site can be easily achieved experimentally than on the metal site, which may interfere with the structural stability of the crystal compound (Lin, Torsi, Geohegan, Robinson, & Xiao, 2021).

In order to determine the structural stability of the doped compounds, phonon dispersion calculation was carried out using Thermo-pw code. Phonons are quasiparticles representing lattice vibrations and their dispersion relations (frequency versus wave vector plots) reveal the crystal's vibrational properties, base on which the stability of the material can be determine.

Mechanical stability can be determine through analysis of elastic constants ( $C_{ij}$ ) of the materials. These constants can be obtained using the energy of the strained system when an applied macroscopic stress is assumed. The energy of the strained crystal compound is given by (Chiodo, Binder, & Bastien, 2011).

$$E_{(V,\varepsilon)} = E_{(V_0,0)} + V_0 \left[ \sum_i \tau_i \varepsilon_i \zeta_i + \frac{1}{2} \sum_{ij} C_{ij} \varepsilon_i \zeta_j \varepsilon_j \zeta_j \right] \quad 1$$

Where  $E_{(V_0,0)}$  is the energy of the unstrained material with equilibrium volume  $V_0$ ,  $\tau_i$  is element in the stress tensor and  $\zeta_i$  is a factor that takes Voigt index into consideration

Since the considered materials are two-dimensional, only two independent elastic constants i.e.  $C_{11}$  and  $C_{12}$  will be considered. The in-plane young modulus (Y) and Poisson ratio ( $\nu$ ) can be calculated using the following expressions

$$Y = \frac{(C_{11}^2 - C_{12}^2)}{C_{11}} \quad 2$$

$$\nu = \frac{C_{12}}{C_{11}} \quad 3$$

The values of the Young modulus (Y) and Poisson ratio ( $\nu$ ) can be analyzed for the mechanical stability of the considered materials. Thermo-pw package was employed for the mentioned calculations

## RESULTS AND DISCUSSION

### Structural properties of single La and Sm atoms doped monolayer NbX<sub>2</sub> (X=S, Se).

Structural properties have a very strong relation with other physical properties, such as electronic, optical, and magnetic properties of the material (Roknuzzaman, Alarco, Wang, & Ostrikov, 2021). In this work, 3 × 3 × 1 supercell of NbSe<sub>2</sub> and NbS<sub>2</sub> monolayer with 27 atoms (9 Nb and 18 S, Se) is taken as the undoped structure. By replacing one Nb atom in the supercell with La atom and later with Sm atom (which is equivalent to 3.7 % dopant concentration) we obtained Figure 1 (doped compounds). Such metallic doping has been carried out with the rear earth atoms for some 2D TMDC (Tian, et, al 2021; Li, et al, 2021).

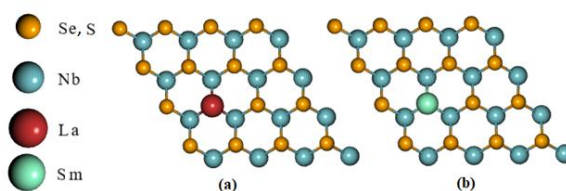


**Figure 1:** Crystal structure of (a) La-doped NbSe<sub>2</sub> and NbS<sub>2</sub> monolayers (b) Sm-doped NbSe<sub>2</sub> and NbS<sub>2</sub> monolayers

In order to get the equilibrium, ground state structural properties of La- and Sm-doped NbSe<sub>2</sub> and NbS<sub>2</sub>, we run structural optimization calculations on the doped materials using GGA PBE. After a geometrical optimization, we observed that both La and Sm we observed that both La and Sm doped compounds maintained the space group of P63/mmc with optimized crystal parameters of  $a = 6.756\text{\AA}$  and  $c = 14.312\text{\AA}$ ,  $a = 6.778\text{\AA}$  and  $c = 14.378\text{\AA}$  in the case of La and Sm doped NbS<sub>2</sub> monolayer, while  $a = 7.226\text{\AA}$  and  $c = 14.848\text{\AA}$  and  $a = 7.259\text{\AA}$  and  $c = 14.808\text{\AA}$  in the case of the doped NbSe<sub>2</sub> monolayer, respectively. Nevertheless, in each we observed a little lattice distortion which leads to an increase on the unit cell along the c-axis due to the La and Sm insertion, similarly in each case there is a volume expansion. The lattice constant is, however, extended slightly in each case. Remarkably, the six La or Sm–S bonds in case of doped NbS<sub>2</sub> monolayer as well as six La or Sm–Se bonds in case of doped NbSe<sub>2</sub> monolayer maintained same length of 2.646 Å and 2.796 Å for doped NbS<sub>2</sub> and NbSe<sub>2</sub> respectively, which means that the inserted La and Sm are located at the center of the octahedron comprising of S and Se atoms, This findings are in excellent agreement with the reported result by (Ugeda et al, 2016; Nakata, et al, 2018; Formo, , et al, 2021; Li, Miao, Wang, & Yang, 2023). Though, it is shorter than those calculated from the effective ionic radii of La, Sm, and S, Se, suggesting a strong covalent hybridization interaction between the rear earth dopants (La, Sm) and the Nb atom, which is similar observed when monolayer NbX<sub>2</sub> (X=S, Se) doped with Sm atom (Liu, et al, 2023). Moreover, the nearest NbSe<sub>6</sub> octahedra around the (La, Sm) are somewhat distorted, which is characterized by the variation of the Nb–S and Nb–Se bond lengths from 2.612Å to 2.646 Å and from 2.638Å to 2.796 Å in case NbS<sub>2</sub> and NbSe<sub>2</sub> respectively.

In order to confirm whether the doped compounds are thermodynamically stable, we calculate the formation energy, which is defined as the difference in total energy of the sum of products minus the sum of the reactants using the expression (Ke et al, 2023).

$$E_{\text{formation}} = E_{\text{doped}} - E_{\text{pure}} - \mu_Y$$

where is  $E_{\text{pure}}$  total energy of the host NbX<sub>2</sub> supercell,  $E_{\text{doped}}$  is the total energy of the doped compound, and  $\mu_Y$  is the chemical potential of the dopants (Y= La and Sm) calculated from their corresponding bulk. The calculated formation energies are given in Table 1.

**Table 1:** Structural Properties of Pure and doped NbSe<sub>2</sub> and NbS<sub>2</sub> monolayers within GGA-PBE Functional

Compound	Bond length (Å)	Bond Angle (°)		Formation Energy (eV)
	D <sub>Nb-</sub> X(X=S,Se)	Θ <sub>Nb-</sub> Se,S-Nb	Θ <sub>Nb-</sub> X(X=S,Se)-Nb	
La-monolayer NbS <sub>2</sub>	2.646	76.10	75.72	-1.688
Sm-monolayer NbS <sub>2</sub>	2.646	77.38	79.17	-1.742
La-monolayer NbSe <sub>2</sub>	2.796	74.67	75.72	-1.821
Sm-monolayer NbSe <sub>2</sub>	2.796	75.38	77.17	-1.899

From the table, it's obvious that the obtained formation energies are all negative, which indicates a thermodynamically stable at ambient conditions and feasible for laboratory synthesis.

#### Effect of La and Sm doping on Mechanical Properties of NbX<sub>2</sub>(X=S, Se) monolayers

Table 2. The results indicate a G/B value of 1.874 and 1.899 for La- and Sm-doped NbS<sub>2</sub> monolayers, respectively, while 1.942 and 1.988 for La- and Sm-doped NbSe<sub>2</sub> monolayers, respectively. Despite these values being a little higher than those obtained in the case of pure NbS<sub>2</sub> and NbSe<sub>2</sub> still the obtained poison ratios for all the doped systems are within the range of mechanically stable (Zhang, Wei, Gao, & Sun, 2020).

**Table 2:** The Bulk modulus, equilibrium Volume (V<sub>0</sub>), and G/B for La and Sm doped monolayer NbSe<sub>2</sub> and NbS<sub>2</sub>

Compounds	B(GPa)	B' <sub>0</sub>	V <sub>0</sub> (a.u. <sup>3</sup> )	G(GPa)	ν	G/B
La-NbS <sub>2</sub>	49.422	4.859	9842.7904	34.335	0.4882	1.874
Sm-NbS <sub>2</sub>	49.866	4.954	9976.8273	35.215	0.5222	1.899
La-NbSe <sub>2</sub>	54.241	4.859	9992.7904	36.404	0.6227	1.942
Sm-NbSe <sub>2</sub>	54.862	4.894	9976.8273	38.664	0.6664	1.988

Similarly, for the calculated independent elastic constants given in Table 3, despite that there is an increase along all the calculated constants but they still obey the Born criteria for a monolayer ( $C_{11} - C_{12} > 0$ ) (Akhter, Kuś, Mrozek, & Burczyński, 2020), which affirmed the mechanical stability of the doped systems.

**Table 3:** Elastic constants (GPa) and Poisson ratio for pure and doped NbSe<sub>2</sub> and NbS<sub>2</sub> monolayers

Elastic Constant (GPa)	Compounds			
	La-NbS <sub>2</sub> Monolayer	Sm-NbS <sub>2</sub> Monolayer	La-NbSe <sub>2</sub> Monolayer	Sm-NbSe <sub>2</sub> Monolayer
C <sub>11</sub>	147.270	149.460	158.220	159.220
C <sub>12</sub>	52.031	54.221	56.284	56.284
C <sub>13</sub>	18.55	19.88	20.200	20.660
C <sub>33</sub>	49.641	49.998	50.125	50.644
C <sub>44</sub>	7.665	9.222	10.125	10.425

#### Conclusion

In summary, RE-doped NbX<sub>2</sub> (X = S, Y) has a substitution-driven behavior. NbX<sub>2</sub> (X = S, Se) is relatively insensitive to atom substitution even at a concentration of 0.48 percent, and these defects may even improve the strain and damage tolerability. These observations have important practical implications for the design of NbX<sub>2</sub> (X = S, Se)-based devices, as doping with heteroatoms is necessary to modulate the NbX<sub>2</sub> (X = S, Se)-band structure without significantly sacrificing its mechanical properties. Even under a void regime, NbX<sub>2</sub> (X = S, Se) can retain a large fraction of its pristine strength and flexibility. Following a direct mapping between Raman parameters and the measured mechanical performance, one can reconcile the relationship between NbX<sub>2</sub> chemical substitutions and structural vacancies and the stiffness, failure strength and behavior of the NbX<sub>2</sub> (X = S, Se). Establishing this relationship between structure and characteristics is also essential for rational design of lattice structures to prevent brittle materials

#### REFERENCES

- Akhter, M. J., Kuś, W., Mrozek, A., & Burczyński, T. (2020). Mechanical properties of monolayer MoS<sub>2</sub> with randomly distributed defects. *Materials*, 13(6), 1307.
- Tian, S., Li, S., Yao, Y., He, M., Chen, L., Zhang, Y., & Zhai, J. (2021). Enhanced electrical performance of monolayer MoS<sub>2</sub> with rare earth element Sm doping. *Nanomaterials*, 11(3), 769.
- Li, Z., Attanayake, N. H., Blackburn, J. L., & Miller, E. M. (2021). Carbon dioxide and nitrogen reduction reactions using 2D transition metal dichalcogenide (TMDC) and carbide/nitride (MXene) catalysts. *Energy & Environmental Science*, 14(12), 6242-6286.
- Roknuzzaman, M., Alarco, J. A., Wang, H., & Ostrikov, K. K. (2021). Structural, electronic and optical properties of lead-free antimony-copper based hybrid double perovskites for photovoltaics and optoelectronics by first principles calculations. *Computational Materials Science*, 186, 110009.

- Roy, S., & Bermel, P. (2018). Electronic and optical properties of ultra-thin 2D tungsten disulfide for photovoltaic applications. *Solar energy materials and solar cells*, 174, 370-379.
- Ugeda, M. M., Bradley, A. J., Zhang, Y., Onishi, S., Chen, Y., Ruan, W., ... & Crommie, M. F. (2016). Characterization of collective ground states in single-layer NbSe<sub>2</sub>. *Nature Physics*, 12(1), 92-97.
- Nakata, Y., Sugawara, K., Ichinokura, S., Okada, Y., Hitosugi, T., Koretsune, T., ... & Sato, T. (2018). Anisotropic band splitting in monolayer NbSe<sub>2</sub>: implications for superconductivity and charge density wave. *npj 2D Materials and Applications*, 2(1), 12.
- Formo, E. V., Hachtel, J. A., Ghafouri, Y., Bloodgood, M. A., & Salguero, T. T. (2021). Thermal stability of quasi-1D NbS<sub>3</sub> nanoribbons and their transformation to 2D NbS<sub>2</sub>: Insights from in situ electron microscopy and spectroscopy. *Chemistry of Materials*, 34(1), 279-287.
- Li, T., Miao, Q., Wang, Y., & Yang, H. (2023). 2D NbS<sub>2</sub> monolayer as a gas sensor for the detection of nitrogen-containing toxic gases. *Surfaces and Interfaces*, 42, 103336.
- Liu, Y., Feng, Y., Hu, L., Wu, X., Qiao, S., & Gao, G. (2023). Structural, electronic phase transitions and thermal spin transport properties in 2D NbSe<sub>2</sub> and NbS<sub>2</sub>: a first-principles study. *Physical Chemistry Chemical Physics*, 25(3), 1632-1641.
- Ke, B., Yang, C., Yao, S., Wei, Q., Ge, S., He, B., ... & Zou, B. (2023). Nickel (II)-Doped Lead-Free Halide Crystals Exhibiting Highly Efficient Tunable Blue-Emitting out of Antiferromagnetic Ni-Ni Coupling. *The Journal of Physical Chemistry Letters*, 14(51), 11597-11602.
- Ostroverkhova, O. (2016). Organic optoelectronic materials: mechanisms and applications. *Chemical reviews*, 116(22), 13279-13412.
- Ding, Y., Wang, Y., Ni, J., Shi, L., Shi, S., & Tang, W. (2011). First principles study of structural, vibrational and electronic properties of graphene-like MX<sub>2</sub> (M= Mo, Nb, W, Ta; X= S, Se, Te) monolayers. *Physica B: Condensed Matter*, 406(11), 2254-2260.
- Rai, A., Movva, H. C., Roy, A., Taneja, D., Chowdhury, S., & Banerjee, S. K. (2018). Progress in contact, doping and mobility engineering of MoS<sub>2</sub>: an atomically thin 2D semiconductor. *Crystals*, 8(8), 316.
- Leonhardt, A., Chiappe, D., Afanas'ev, V. V., El Kazzi, S., Shlyakhov, I., Conard, T., ... & De Gendt, S. (2019). Material-selective doping of 2D TMDC through Al x O y encapsulation. *ACS applied materials & interfaces*, 11(45), 42697-42707.
- Ryder, C. R., Wood, J. D., Wells, S. A., & Hersam, M. C. (2016). Chemically tailoring semiconducting two-dimensional transition metal dichalcogenides and black phosphorus. *ACS nano*, 10(4), 3900-3917.
- Yang, F., Hu, P., Yang, F. F., Chen, B., Yin, F., Sun, R., ... & Yin, Z. (2023). Emerging enhancement and regulation strategies for ferromagnetic 2D transition metal dichalcogenides. *Advanced Science*, 10(21), 2300952.
- Tedstone, A. A., Lewis, D. J., & O'Brien, P. (2016). Synthesis, properties, and applications of transition metal-doped layered transition metal dichalcogenides. *Chemistry of Materials*, 28(7), 1965-1974.
- Li, S., Tian, S., Yao, Y., He, M., Chen, L., Zhang, Y., & Zhai, J. (2021). Enhanced electrical performance of monolayer MoS<sub>2</sub> with rare earth element Sm doping. *Nanomaterials*, 11(3), 769.
- Khan, U., Ali, B., Ullah, H., Idrees, M., Nguyen, C., & Amin, B. (2024). Tuning the electronic structure and Schottky barrier by NbX<sub>2</sub> contact to MXY (M= Mo, W; (X≠ Y) S, Se, Te) monolayer. *Micro and Nanostructures*, 187, 207765.
- Iqbal, M. W., Elahi, E., Amin, A., Hussain, G., & Aftab, S. (2020). Chemical doping of transition metal dichalcogenides (TMDCs) based field effect transistors: A review. *Superlattices and Microstructures*, 137, 106350.
- Moeller, T., & Kremers, H. E. (1945). The Basicity Characteristics of Scandium, Yttrium, and the Rare Earth Elements. *Chemical Reviews*, 37(1), 97-159.
- Atwood, D. A. (Ed.). (2013). *The rare earth elements: fundamentals and applications*. John Wiley & Sons.
- Braud, A. (2010). Excitation mechanisms of re ions in semiconductors. In *Rare Earth Doped III-Nitrides for Optoelectronic and Spintronic Applications* (pp. 269-307). Dordrecht: Springer Netherlands.
- Malik, M., Iqbal, M. A., Choi, J. R., & Pham, P. V. (2022). 2D materials for efficient photodetection: overview, mechanisms, performance and UV-IR range applications. *Frontiers in Chemistry*, 10, 905404.
- Rani, R., & Sinha, M. M. (2024). Recent advances in two-dimensional transition metal oxides and dichalcogenides as efficient thermoelectric materials. *Physica Scripta*, 99(3), 032002.
- Yoo, H., Heo, K., Ansari, M. H. R., & Cho, S. (2021). Recent advances in electrical doping of 2D semiconductor materials: Methods, analyses, and applications. *Nanomaterials*, 11(4), 832.
- Zhang, C., Wei, N., Gao, E., & Sun, Q. (2020). Poisson's ratio of two-dimensional hexagonal crystals: A mechanics model study. *Extreme Mechanics Letters*, 38, 100748.